Modern Applied Science; Vol. 12, No. 9; 2018
ISSN 1913-1844 E-ISSN 1913-1852
Published by Canadian Center of Science and Education

RHF and DFT Study of the Molecular and Electronic Properties of $(SiO_2)_n$ and $(GeO_2)_n$ Nanoclusters

Chifu E. Ndikilar[1], L. S. Taura[2], G. W. Ejuh[3,4] & A. Muhammad[1]

[1] Department of Physics, Federal University Dutse, Jigawa State, Nigeria

[2] Department of Physics, Sule Lamido University Kafin-Hausa, Jigawa State, Nigeria

[3] University of Bamenda, National Higher Polytechnic Institute, Departmet of Electrical and Electronic Engineering, P. O. Box 39 Bambili, Cameroon

[4] University of Dschang, IUT-FV of Bandjoun, Department of General and Scientific Studies, West Cameroon

Correspondence: Chifu E. Ndikilar, Physics Department, Sule Lamido University, P.M.B 048, Kafin Hausa, Jigawa State, Nigeria. Tel: 234-8034-512-189. E-mail: ebenechifu@yahoo.com, lawansani21@gmail.com

Received: April 24, 2018 Accepted: June 5, 2018 Online Published: August 16, 2018

doi:10.5539/mas.v12n9p108 URL: https://doi.org/10.5539/mas.v12n9p108

The research is financed by Tertiary Education Trust Fund (TET Fund), Nigeria.

Abstract

The study of nanoclusters has attracted a lot of scientific research over the years. This class of materials are important because they bridge the gap between bulk materials and molecular structures. Silicon and Germanium oxides have many applications in semiconductor technology and nanotechnology. In this research work, molecular and electronic properties of Silicon and Germanium dioxide nanoclusters are studied. The results obtained reveal the comparative advantages and disadvantages of using any of the two oxides for particular applications. Restricted Hartree Fock and Density Functional Theory computations of the molecular and electronic properties of $(SiO_2)_n$ and $(GeO_2)_n$ nanoclusters (n = 1,..,6) are studied. Silicon dioxide clusters are found to have higher thermal energies and lower average bond lengths and are thus more stable than Germanium dioxide clusters. At n = 1, both nanoclusters are non-polar, but gradually become more polar with increase in n. The average polarizability, molecular hyperpolarizability and total thermal energies of the nanoclusters increases with increase in molecular size. Computed values of the electron affinities for $(SiO_2)_n$ clusters agree with experimental results. Some of the most intense Infra Red vibrational motions observed in both molecules are anti-symmetric stretching of Si=O/Ge-O and chain in plane, symmetric stretching of the Si=O/Ge-O bonds and chain in plane and symmetric twisting/breathing of the chain(s) in plane. The two nanoclusters are also Raman active at some frequencies.

Keywords: electronic, germanium, silicon, nanoclusters, oxides

1. Introduction

Silicon (Si) and Germanium (Ge) are two Group IV elements which crystallize in the diamond cubic crystal structure. Germanium, unlike Silicon, does not exist in its pure form on Earth. Silicon dioxide is one of the most common compounds on Earth. Silicon and Germanium dioxides exist in crystalline and amorphous phases. Germanium dioxide unlike Silicon dioxide is soluble in water. (Janke, 2008).

Silicon dioxide is suitable for the fabrication of semiconductor devices due to its chemical stability and good electrical insulation properties. Also, Silicon dioxide nanoparticles have high surface areas which are highly desirable as catalytic support (Sahnoun *et al*, 2005). Silicon and its compounds have dominated the semiconductor industry over the years for a number of reasons. Firstly, the existence of a stable Silicon oxide which serves as a dielectric on device surfaces has played an important role in favor of Silicon. Secondly, the scarcity and cost of Germanium has also favored the dominance of Silicon. However, with recent advances in semiconductor technology, the use of SiO_2 as a dielectric is becoming challenging. This is due to the fact that as the dielectric thickness reduces, it approaches the point where electron tunneling becomes an important effect (Janke, 2008).

Germanium is being considered extensively as an alternative desirable material. This is because of its higher low field mobility - a factor of two higher for electrons and four for holes compared with Silicon. Germanium dioxide

is similar to Silicon dioxide in many aspects and occurs in three stable forms at ambient temperature (Ivana *et al*, 2014). The properties of Germanium are less understood compared to those of Silicon. This is largely due to the dominance of Silicon technology for the past decades and difficulties in transferring techniques which have been very successful in Silicon to Germanium. Problems have also been encountered in modeling Germanium and its oxides. Despite these problems, the study of Germanium compounds and its defects is an area of active research interest (Lee, 2007).

Nanoparticles attract much scientific interest as they effectively bridge the gap between bulk materials and atomic or molecular structures. Group-IV nanocrystals have emerged as a promising group of materials that extends the realm of application of bulk diamond, Silicon, Germanium and related materials beyond their traditional boundaries. Over the last two decades of research, their potential for application in areas such as optoelectronics and memory devices has been progressively unraveled. Silicon dioxide thin films have been used extensively in electronics, optics and surface treatment fields. Also, Silicon nanoparticles have good potentials for biochemical applications in controlled drug delivery and tissue engineering (Nikolaos *et al*, 2016).

In view of the importance of these nanoparticles, it is imperative to carry out a comparative study of the two oxides. This study is aimed at revealing the comparative advantages and disadvantages of using any of the two oxides for particular applications. RHF and DFT are used to carry out a comparative analysis of the structural, electronic and vibrational properties of some small Silicon and Germanium dioxide nanoclusters.

2. Methods

The windows version of Gaussian 9W Revision A.02-SMP is used. Geometry optimization is carried out at Restricted Hartree Fock (RHF) and Density Funtional Theory (DFT) levels of theory. Geometry optimizations locate minima on the potential energy surface, thus predicting equilibrium structures of the molecular systems. The input molecular structures are built using GaussView 5.0.8 (Frisch *et al*, 2009).

The structures are completely optimized and studied at the RHF level of theory using the basis set 6-31G(d,p). The molecules are then studied at DFT level of theory using Becke 3 Lee Yarr Parr (B3LYP) method which is a cost effective method for inclusion of electron correlations with the same basis set (Gurku & Ndikilar, 2012; Galadanci *et al*, 2015). The DFT method has proven to be one of the most accurate methods for the computation of the electronic structure of solids (Jamal, 2014). In addition, vibrational frequencies for optimized molecular structures are also calculated. The optimized geometry of the molecules has no imaginary vibrational frequencies which imply that minimum potential energy is found for each molecule.

The Highest Occupied Molecular Orbital (HOMO) and Lowest Unoccupied Molecular Orbital (LUMO) energies are extracted from the eigenvalues and used to compute the Ionization Potential (IP), Electron Affinity (EA), energy band gap (or global hardness) E_g, chemical potential(μ), chemical hardness (η) and electrophilicity index (ω) (Taura *et al*, 2017).

3. Results and Discussion

3.1 Optimized Molecular Structures

The optimized structures are shown in Fig.1. The stable optimized structures of Silicon oxides have two double linear bonds between Silicon atoms and Oxygen atoms; unlike the Germanium oxides that have single linear bonds. Fig. 1 shows that small silicon oxide and Germanium oxide clusters can exist as ring or chain structures. It is expected that as the cluster size increases other three dimensional structures may occur with more structural isomers (Yuhai & Tersoff, 1999). The mean optimized bond lengths for the common bonds in both nanocluster types are computed and presented in Table 1.

Table 1. Mean Optimized Bond Lengths (Å)

n	$(SiO_2)_n$				$(GeO_2)_n$			
	RHF/6-31G(d, p)		B3LYP/6-31G(d, p)		RHF/6-31G(d, p)		B3LYP/6-31G(d, p)	
	Si-O	Si=O	Si-O	Si=O	Linear Ge-O	Chain Ge-O	Linear Ge-O	Chain Ge-O
1	-	1.4824	-	1.5198	1.6020	-	1.6416	-
2	1.6489	1.4807	1.6815	1.5141	1.6060	1.7717	1.6392	1.8166
3	1.6481	1.4813	1.6779	1.5140	1.6055	1.7683	1.6381	1.8096
4	1.6314	1.4594	1.6680	1.5153	1.6053	1.7670	1.6375	1.8074
5	1.6481	1.4818	1.6763	1.5145	1.6059	1.7660	1.6382	1.8060
6	1.6482	1.4819	1.6762	1.5144	1.6060	1.7667	1.6380	1.8055

Table 1 shows that the mean Si-O bonds are longer and hence weaker than the side Si=O bonds. The change in mean bond length with molecular size is very insignificant. The mean bond length of Si-O at both levels of theory best agree with the experimental value of 1.6 Å (Yuhai & Tersoff, 1999). At B3LYP level of theory, greater mean bond lengths are predicted for both nanoclusters. The Ge-O bonds within the sub chains in the nanoclusters are longer and weaker than the linear side Ge-O bonds. The chain Ge-O bonds within the sub chains are longer compared to the equivalent Si-O chains. Thus, from the values of the mean bond lengths, it can be concluded that Silicon dioxide nanoclusters are more stable than those of Germanium. X-ray diffraction gives the Ge-O bond length as 1.74 Å (Micoulaut *et al*, 2006) which agrees with values obtained in Table 1.

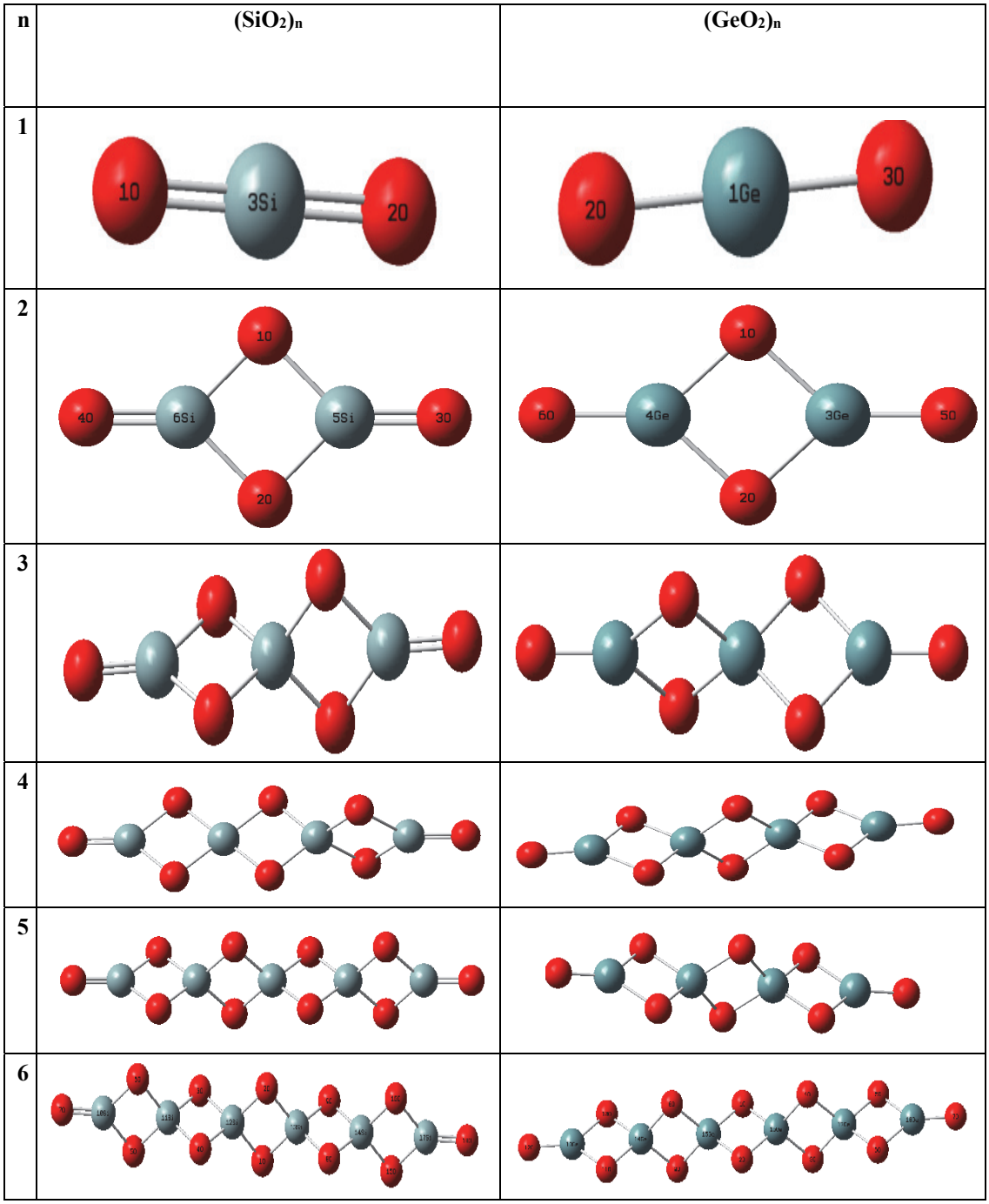

Figure 1. Optimized Structures of the Nanocluster Molecules

3.2 Dipole Moments, Quadrupole Moments, Polarizabilities and Total Thermal Energies

The first derivative of the energy with respect to an applied electric field gives the dipole moments of the molecules.

It is given as a three-dimensional vector in the Gaussian output file and is a measure of asymmetry in the molecular charge distribution (Robertson, 2004). Total dipole moments (μ) are shown in Table 2. It is deduced from Table 2 that both nanoclusters at n=1 are non polar, but gradually become more polar with increase in n. Also, RHF values are slightly lower than B3LYP values.

The total thermal energies (E_0), averages polarizability (<α>) and molecular hyperpolarizability (β_{mol}) of the clusters at both levels of theory are also computed and presented in Table 2. These molecular properties are essential in understanding many physical phenomena, molecular simulation and modeling of fundamental processes, search of new optical materials and thermodynamic properties of molecules. The relationship between the molecular structure and non-linear optical properties of molecules can be deduced from hyperpolarizability values. Hyperpolarizability is a measure of the nonlinear optical activity of a molecule and thus molecules with large values can produce second order optical effects (Ejuh & Ndjaka, 2013). Accurate knowledge of atomic polarizabilities is very important in many applications including development of the next-generation atomic time and frequency standards, optical cooling and trapping schemes, quantum information with neutral atoms, study of fundamental symmetries, thermometry and other macroscopic standards, study of cold degenerate gases, study of long-range interactions, atomic transition rate determinations, and benchmark comparisons of theory and experiment.

Table 2. Dipole Moments, Average Polarizabilities, Hyperpolarizabilities and Total Thermal Energies

Nanocluster	Method	n	μ(Cm) $x10^{-33}$	<α>(esu) $x10^{-12}$	β_{mol} (esu) $x10^{-33}$	Kcal/mol E_0
$(SiO_2)_n$	RHF/6-31G(d,p)	1	0.00	2.82	375.50	6.803
		2	17.00	5.13	802.98	15.728
		3	2.00	7.46	1226.11	24.920
		4	6.00	11.65	1989.26	30.840
		5	7.33	12.24	2090.14	43.710
		6	13.33	14.66	2526.89	52.883
	B3LYP/6-31G(d,p)	1	0.00	3.42	363.19	6.337
		2	58.33	6.37	770.94	14.643
		3	6.33	9.27	1175.45	23.297
		4	5.67	14.64	1671.53	28.619
		5	14.33	15.31	1997.16	40.937
		6	55.66	18.37	2411.35	49.586
$(GeO_2)_n$	RHF/6-31g(d,p)	1	0.00	4.06	450.20	5.770
		2	1.00	6.67	942.11	13.592
		3	21.33	9.80	1450.98	22.132
		4	10.67	12.99	1956.12	29.946
		5	15.67	16.21	2461.60	38.531
		6	31.33	19.46	2969.22	46.677
	B3LYP/6-31G(d,p)	1	0.00	4.00	303.92	5.493
		2	12.00	8.11	906.94	12.735
		3	22.33	12.19	1378.19	20.674
		4	15.33	16.41	1853.20	28.010
		5	19.67	20.72	2329.36	35.986
		6	39.33	25.09	2807.48	43.583

It can be observed from Table 2 that the average polarizability and molecular hyperpolarizability of the nanoclusters increases as n increases. The corresponding B3LYP values of polarizability are greater than the RHF values. This shows that as the molecular size increases, the potential of the molecules to have non-linear optical properties also increases. The values obtained for the polarizability of SiO_2 are higher compared to those obtained from *ab initio* coupled perturbed Hartree–Fock (CPHF) method (Bacskay, 1983). Table 2 shows large values of hyperpolarizability and thus these nanoclusters can serve as good Non-Linear Optical (NLO) materials. Important parameters influencing hyperpolarizability include donor–acceptor system, nature of substituents, conjugated π system and the influence of planarity (Arulmozhi & Madhavan , 2015).

Table 2 shows that total thermal energy decreases from RHF to B3LYP for both nanocluster molecules. Hence,

inclusion of electron correlation brings a reduction in total thermal energies. The thermal energies also increase with increase in the size of the molecules. Generally, the Silicon dioxide clusters have higher thermal energies compared to Germanium. Hence, they are more stable, as earlier deduced from the mean bond lengths.

Quadrupole moments (Table 3) are second order approximations of the total electron distribution and give an approximate idea of the molecular shape.

Table 3. Quadrupole Moments of the Molecules (Debye-Ang)

Nanocluster	**n**	RHF/6-31G(d,p)			B3LYP/6-31G(d,p)		
		XX	YY	ZZ	XX	YY	ZZ
$(SiO_2)_n$	1	-19.03	-19.03	-34.13	-19.75	-19.75	-31.42
	2	-70.24	-47.75	-37.53	-64.79	-47.49	-38.86
	3	-106.39	-66.42	-66.42	-97.97	-66.76	-66.76
	4	-153.39	-104.89	-91.45	-135.70	-102.85	-91.88
	5	-180.47	-113.94	-113.93	-165.84	-113.88	-113.88
	6	-218.11	-142.80	-132.61	-200.20	-141.76	-133.15
$(GeO_2)_n$	1	-23.76	-23.76	-39.83	-24.513	-24.51	-36.07
	2	-81.32	-57.87	-46.93	-73.59	-57.05	-48.48
	3	-122.46	-81.28	-81.27	-110.68	-81.24	-81.23
	4	-164.13	-115.61	-104.70	-148.01	-113.98	-105.43
	5	-206.24	-139.02	-139.01	-185.79	-138.18	-138.15
	6	-248.60	-173.36	-162.44	-223.67	-170.92	-162.36

Table 3 shows that the molecules are slightly elongated along XX axis, with increase in elongation as the size of the molecule increases for n = 2,...,6. For n = 1, the molecules are slightly elongated along the ZZ axis. Electron correlation slightly reduces the molecular elongation. The average quadrupole moments at RHF level of theory for SiO_2 (-24.15 Debye-Ang) and GeO_2 (-29.12 Debye-Ang) are higher than that of Carbon dioxide (Battaglia *et al*, 1981).

3.4 Electronic Properties and Reactivity Indices

Large values of HOMO and LUMO energies play an important role in the electronic, optical and chemical properties of molecules (Ejuh *et al*, 2017). Electronic systems with larger HOMO-LUMO energy band gap (E_{gap}) are less reactive compared to those with a smaller band gap (Arjunan *et al*, 2011). The Ionization Potential (IP), Electron Affinity (EA) , energy band gap (or global hardness) E_g, chemical potential, μ , chemical hardness η , and electrophilicity index ω are calculated and shown in Table 4

Table 4. Electronic Properties and Reactivity Indices

Nanocluster	**Method**	**n**	IP **(eV)**	EA **(eV)**	E_g **(eV)**	μ **(eV)**	η **(eV)**	ω **(eV)**
$(SiO_2)_n$	RHF/6-31G(d,p)	1	1.36888	-0.03510	1.40398	-0.66689	0.70199	0.15610
		2	1.36322	-0.03921	1.40243	-0.66201	0.70122	0.15366
		3	1.36376	- 0.0775	1.44123	-0.64315	0.72062	0.14904
		4	1.37568	0.07673	1.29894	-0.72621	0.64947	0.17126
		5	1.35296	-0.11143	1.46439	-0.62077	0.73220	0.14108
		6	1.34986	- 0.1200	1.46988	-0.61492	0.73494	0.13895
	B3LYP/6-31G(d,p)	1	0.92145	0.35426	0.56522	-0.63786	0.28261	0.05749
		2	1.08515	0.53529	0.54985	-0.81022	0.27493	0.09024
		3	0.92155	0.30931	0.61225	-0.61543	0.30613	0.05797
		4	0.94120	0.43709	0.50411	-0.68915	0.25206	0.05986
		5	1.05407	0.47012	0.58395	-0.76210	0.29198	0.08479
		6	0.90975	0.27453	0.63521	-0.59214	0.31761	0.05568
$(GeO_2)_n$	RHF/6-31G(d,p)	1	1.31554	-0.07602	1.39157	-0.61976	0.69579	0.13363
		2	1.31301	-0.03309	1.34610	-0.63996	0.67305	0.13782
		3	1.31769	-0.04552	1.36322	-0.63609	0.68161	0.13789

	4	1.31293	-0.05418	1.36711	-0.62938	0.68356	0.13534
	5	1.31037	-0.06044	1.37081	-0.62497	0.68541	0.13386
	6	1.30809	-0.06489	1.37299	-0.62160	0.68650	0.13262
B3LYP/6-	1	0.87932	0.327267	0.55206	-0.60329	0.27603	0.05023
31G(d,p)	2	0.87258	0.359104	0.51347	-0.61584	0.25674	0.04869
	3	0.88161	0.355049	0.52656	-0.61833	0.26328	0.05033
	4	0.87752	0.351076	0.52645	-0.61430	0.26322	0.04967
	5	1.00126	0.43845	0.56281	-0.71986	0.28141	0.07291
	6	0.87472	0.34585	0.52887	-0.61029	0.26444	0.04925

Table 4 shows that the RHF method predicts slightly higher values for the Ionization Potential (IP) and Energy band gap compared to the B3LYP method. Computed values of the electron affinities for $(SiO2)_n$ clusters agree with experimental results observed at 4.66 eV photon energy (Robertson, 2004). However, the observed electron affinities within the range 4.0 - 4.5 eV for the GeO_2/Ge interface differs from the computed values. This could be due to the contribution from the interface. The computed energy band gaps for Silicon and Germanium dioxide nanoclusters are lower compared to experimental values. However, the predicted band gaps of the nanoclusters are comparable to those of the elements, Germanium (0.66 eV) and Silicon (1.12 eV) (Ay & Aydinli, 2004) .

The chemical potential and chemical hardness are key indicators of the overall reactivity of a molecule and are the most fundamental descriptors of charge transfer during a chemical reaction. The nature of electronegativity, hardness and the electrophilicity index are fundamentally qualitative descriptors as they are not observable. They occur but cannot be seen. Hence, the possibility of experimental determination of such descriptors is not yet possible (Nazmul & Dulal, 2012). The predicted chemical potentials do not change with increase in nanocluster size at both levels of theory. This shows that if there is an interface between any two nanoclusters in Table 4, there will be no significant flow of particles between them. RHF predicts far more higher values for chemical hardness for both molecules compared to DFT. This suggest that the neglect of electron correlation in the computational method erroneously depicts a higher resistance to change in electron distribution. Electrophilicity is an intrinsic property of molecules and signifies the energy lowering process on soaking electrons from donors (Nazmul & Dulal, 2012). The electrophilicity index measures the stabilization in energy when the system acquires an additional electronic charge from the environment. The computed electrophicity index for the nanoclusters are not significantly different for both nanoclusters at both levels of theory.

3.5 Electrostatic Potential Derived Charges

The mean electrostatic potential derived charges using the CHelpG scheme of Breneman are computed and shown in Table 5. These charges can be used to study electrostatic interaction energies in the different molecules. Electrostatic potential maps for a given molecule explicitly show regions of electronegativity and electropositivity that are not easily inferred from inspection of the parent charge density distribution. From a potential map, energetically favorable Coulombic interactions of a molecule with its neighbors can readily be understood, since these will involve the overlap of electropositive with electronegative regions, to give at least a partial cancellation (Stewart & Craven, 1993).

Table 5. Mean Electrostatic Potential Derived Charges on different atoms

n	**$(SiO_2)_n$**				**$(GeO_2)_n$**			
	RHF/6-31G(d, p)		**B3LYP/6-31G(d, p)**		**RHF/6-31G(d, p)**		**B3LYP/6-31G(d, p)**	
	Si	O	Si	O	Ge	O	Ge	O
1	1.264757	-0.632378	0.950423	-0.475211	1.496560	-0.748280	1.141633	-0.570816
2	1.383725	-0.691863	1.034084	-0.517042	1.556195	-0.747875	1.127695	-0.563847
3	1.439765	-0.719883	1.076988	-0.538493	1.624682	-0.812341	1.206259	-0.603133
4	1.491125	-0.745562	1.089062	-0.594531	1.655614	-0.827807	1.187429	-0.593714
5	1.494880	-0.747440	1.121364	-0.560682	1.674502	-0.837218	1.198165	-0.537027
6	1.509132	-0.754566	1.254990	-0.566618	1.686429	-0.843214	1.204615	-0.602307

The bulk positive charge in both molecules resides with the Silicon or Germanium atoms and negative charge resides mainly with the Oxygen atoms as expected. This is due to the high electro-negativity of the Oxygen atoms. B3LYP values for both molecules are slightly lower in magnitude. Also, the Germanium oxides have higher mean

electrostatic potential derived charges. It is noticed that O atoms in the chain are slightly more electronegative than those at the sides (Ejuh *et al*, 2015).

3.6 Vibrational Frequencies and Assignments

The vibrational spectra of nanoclusters at ground state were also predicted. These frequency calculations are valid only at stationary points on the potential energy surface, thus our computations were performed on the optimized structures of the molecules. Infra Red and Raman intense vibration frequencies and spectra are determined at both levels of theory.

Raw frequency calculations computed at the Hartree-Fock level contain known systematic errors due to the neglect of electron correlation, resulting to overestimates of about 10-12%. Therefore, it is usual to scale frequencies predicted at the HF level by an empirical factor of 0.8929. Use of this factor has been demonstrated to produce very good agreement with experiment for a wide range of systems. Our values in this study must be expected to deviate even a bit more from experiment because of the choice of a medium-sized basis set around . For B3LYP , a scale factor of 0.9613 is used (Frisch *et al*, 2009).

Table 6 and 7 show respectively some common intense IR and Raman vibrational frequencies for the clusters.

Table 6. Some Common IR Intense Vibrational Frequencies (cm^{-1})

(a) Anti-symmetric stretching of Si=O/Ge-O and chain in plane

n	**$(SiO_2)_n$**		**$(GeO_2)_n$**	
	RHF/6-31G(d,p)	B3LYP/6-31G(d,p)	RHF/6-31G(d,p)	B3LYP/6-31G(d,p)
1	1603.67	1449.34	210.49	170.30
2	1445.53	1313.01	800.09	688.34
3	735.34	819.15	832.38	720.37
4	226.3	324.21	816.80	773.39
5	1049.44	959.63	804.29	697.63
6	1148.28	1060.26	845.55	736.21

(b) Symmetric stretching of the Si=O/Ge-O bonds and chain in plane

n	**$(SiO_2)_n$**		**$(GeO_2)_n$**	
	RHF/6-31G(d,p)	B3LYP/6-31G(d,p)	RHF/6-31G(d,p)	B3LYP/6-31G(d,p)
1	328.99	262.73	111.46	1027.58
2	876.38	777.83	1065.15	977.09
3	659.22	288.53	1102.46	1013.19
4	216.70	243.17	1076.92	989.87
5	945.82	818.11	823.71	715.51
6	1023.28	938.02	836.80	708.19

(c) Symmetric twisting of the chain(s) in plane

n	**$(SiO_2)_n$**		**$(GeO_2)_n$**	
	RHF/6-31G(d,p)	B3LYP/6-31G(d,p)	RHF/6-31G(d,p)	B3LYP/6-31G(d,p)
1	-	-	-	-
2	990.68	898.81	788.14	707.98
3	330.53	431.67	823.58	814.07
4	220.78	356.11	806.01	728.59
5	1033.27	948.74	836.63	777.23
6	1035.28	951.87	862.44	695.46

(d) Twisting of the chain(s) out of plane

n	**$(SiO_2)_n$**		**$(GeO_2)_n$**	
	RHF/6-31G(d,p)	B3LYP/6-31G(d,p)	RHF/6-31G(d,p)	B3LYP/6-31G(d,p)
1	-	-	-	-
2	520.33	431.90	356.54	286.83

3	506.91	600.93	730.74	745.47
4	441.12	396.98	796.72	690.54
5	1029.58	866.33	888.79	736.87
6	1030.51	853.79	920.50	769.96

The computed IR vibrations for Silicon dioxide agree with experimental work as twisting, anti-symmetric bending and symmetric stretching are observed respectively at 448 cm^{-1}, 826 cm^{-1}, 1026 cm^{-1} (Wang *et al*, 1996). Fig. 2 shows some selected IR spectra for the studied molecules. The similarity between the spectra of both molecules at a given n is clearly shown in Fig. 2 with similar peaks. Experiments have shown that the IR spectra of GeO_2 has two prominent peaks at 560 cm^{-1} and 870 cm^{-1}, corresponding to asymmetric stretching of the Ge-O bonds (Micoulaut *et al*, 2006).

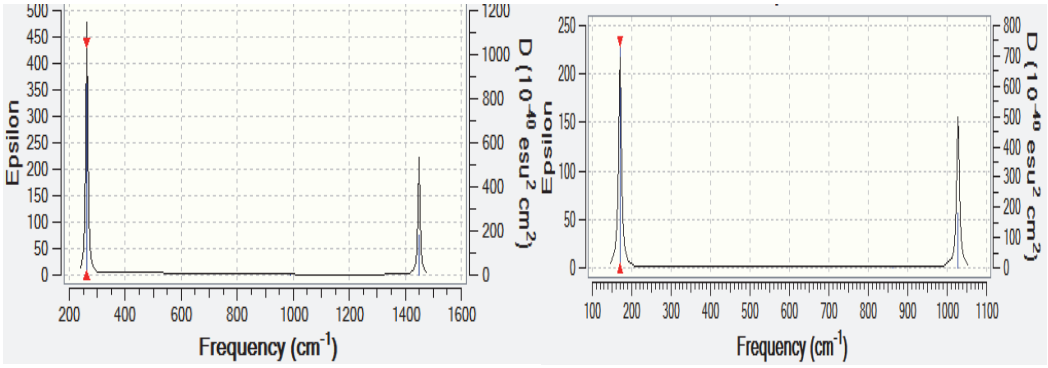

(a) SiO_2 (b) GeO_2

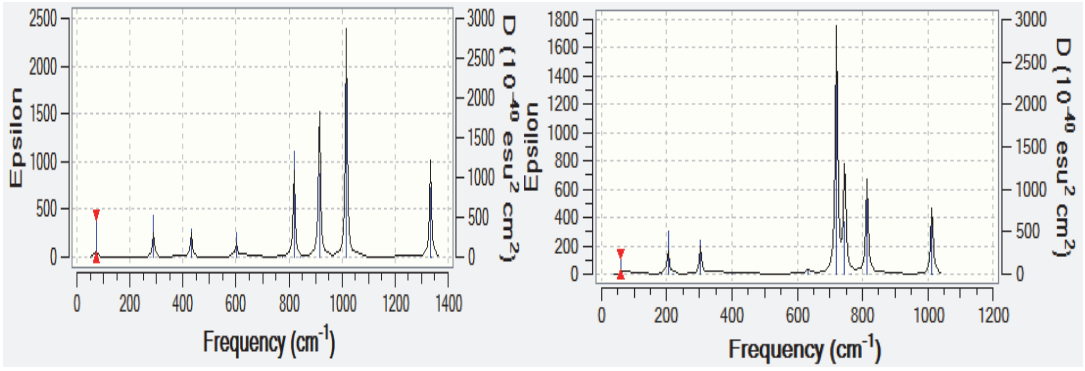

(c) $(SiO_2)_3$ (d) $(GeO_2)_3$

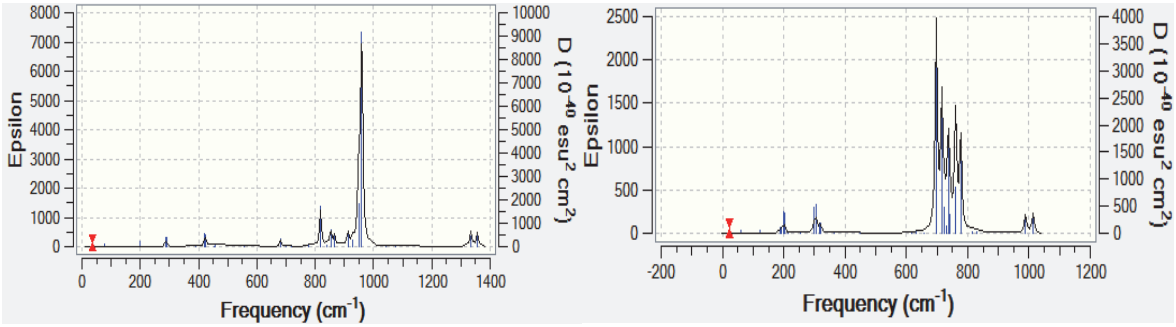

(e) $(SiO_2)_5$ (f) $(GeO_2)_5$

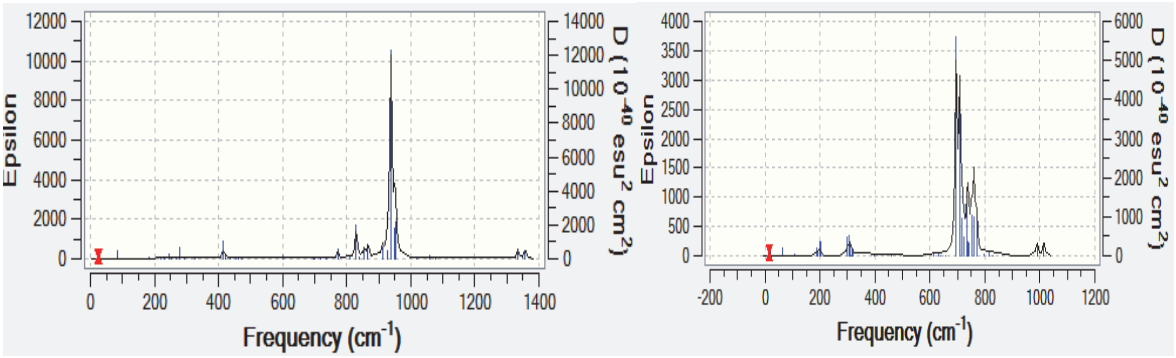

(g)$(SiO_2)_6$ (h) $(GeO_2)_6$

Figure 2. Some Sampled IR Spectra at B3LYP

Table 7. Some common Raman Intense Vibrational Frequencies (cm^{-1})

(a) Si=O/Ge-O linear bond symmetric stretching in plane

n	$(SiO_2)_n$		$(GeO_2)_n$	
	RHF/6-31G(d,p)	B3LYP/6-31G(d,p)	RHF/6-31G(d,p)	B3LYP/6-31G(d,p)
1	1111.02	990.87	960.51	861.64
2	1231.11	1350.98	1076.07	987.16
3	214.15	325.36	1105.65	1015.47
4	257.35	229.14	1078.06	990.85
5	974.62	839.44	888.79	758.60
6	945.32	866.47	862.44	715.25

(b) Symmetric twisting of chain

n	$(SiO_2)_n$		$(GeO_2)_n$	
	RHF/6-31G(d,p)	B3LYP/6-31G(d,p)	RHF/6-31G(d,p)	B3LYP/6-31G(d,p)
1	-	-	-	-
2	602.91	848.60	865.58	743.29
3	506.92	774.75	885.92	766.80
4	139.34	231.88	855.09	741.45
5	945.82	853.20	870.86	777.23
6	937.32	840.09	883.82	769.96

Popovic *et al*. (2011) observed intense Raman peaks for SiO_2 at 521 cm^{-1} and 1100 cm^{-1}. Experiments show that the Raman spectra of crystalline polymorphs of GeO_2 have three strong peaks at 173 cm^{-1}, 701 cm^{-1} and 873cm^{-1} corresponding respectively to asymmetric stretching of Ge-O-Ge bonds, Oxygen breathing and symmetric stretching twisting of bonds. This agrees with the common vibrations observed in this work.

4. Conclusion

The mean bond lengths and total thermal energies predict that Silicon dioxide clusters are more stable than the corresponding Germanium dioxides. The polarity of the molecules increases with increase in size. The quadrupole moments and polarizabilities of the two types of nanoclusters were also studied. There is a great similarity in the electronic properties of the two nanocluster molecules. The bulk positive charges reside mainly with the Silicon and Germanium atoms and the highly electronegative Oxygen atoms carry the bulk negative charge.

It would be interesting to study and determine the structural diversification of the nanoclusters. The chain and linear structures can be examined to see which are more stable and have more favorable electronic and molecular properties for use. Also, understanding of the structural hierarchy of the small silicon and germanium oxide clusters will provide good models to test theories and help in understanding the bulk properties of many materials based on these oxides. This understanding may also aid the design of new materials with novel structural building blocks which may have many applications in nanotechnology.

Acknowledgments

We acknowledge that this research project was sponsored by the Tertiary Education Trust Fund (TET Fund), Nigeria through the Institution Based Research (IBR) intervention, 2017.

References

Arjunan, V., Balamourougane, P. S., Mythili, C. V., & Mohan, S. (2011). Vibrational, nuclear magnetic resonance and electronic spectra, quantum chemical investigation of 2-amino 6 flourobenzothiazole. *Journal of Molecular Structure, 1006*(3)*,* 247-256. https://doi.org/10.1016/j.molstruc.2011.09.015

Arulmozhi, S., & Madhavan, J. (2015). Molecular structure, first-order hyperpolarizability and HOMO-LUMO studies of L-Histidinium Dinitrate. *IOP Conf. Series: Materials Science and Engineering, 73*, 012035. https://doi.org/10.1088/1757-899X/73/1/01203

Ay, F., & Aydinli, A. (2004). Comparative investigation of hydrogen bonding in silicon based PECVD grown dielectrics for optical waveguides. *Optical Materials, 26*, 33-46. https://doi.org/10.1016/j.optmat.2003.12.004

Bacskay, G. G. (1983). An *ab initio* SCF calculation of the polarizability tensor of sulphur dioxide. *The Journal ofChemical Physics,79*, 2090. https://doi.org/10.1063/1.445997

Battaglia, M. R., Buckingham, A. D., Neumark, D., Pierens, K., & Williams, J. H. (1983). The quadrupole moments of carbon dioxide and carbon disulphide. *Molecular Physics*, *43*, 1015-1020. https://doi.org/10.1080/00268978100101831

Ejuh, G. W., & Ndjaka, J. M. (2013). Linear and non linear optical effects of Pyrimethamine and Sulfadoxine: AB initio and density functional study. *The African Review of Physics, 8*, 463-475.

Ejuh, G. W., Nouemo, S., Ndikilar, C. E., Nya, F. T., & Marie N. J. (2015). Vibrational spectra, electronic structure and properties of the molecules Aspirin and Ibuprofen. *Journal of Advances in Physics, 10*(2), 2696-2714. https://doi.org/10.24297/jap.v10i2.1331

Ejuh, G. W., Ottou, A. M. T., Tchangwa, N. F., &Ndjaka, J. M. B (2017). Prediction of electronic structure, dielectric and thermodynamical properties of Fluibiprofen by Density Functional Theory calculation. *Karbala Journal of Modern Sciences*, *10*. https://doi.org/1016/j.kijoms.2017.10.001

Frisch, M. J., Trucks, G. W., Schlegel, H. B., Scuseria, G. E., Robb, M. A., … Pople, J. A. (2009). Gaussian, Inc., Wallingford CT Gaussian 09, Revision A.

Galadanci, G. S. M., Ndikilar, C. E., Sabiu, S. A., & Safana, A. (2015). Molecular dynamics and vibrational analysis of pentacene: RHF and DFT study. *Chemistry & Materials Research*, *7*(11), 16 - 23.

Gurku, U., & Ndikilar, C. E. (2012). Electronic structure and properties of the organic semi conductor material Anthracene in gas phase and ethanol: an ab Initio and DFT study. *The African Review of Physics, 7*, 253-263.

Ivana, C., Carvalho A., & Coutinho, J. (2012). Silicon and Germanium nanocrystals: properties and characterizaation. *J. Nanotechnol, 5*, 1787-1794. https://doi.org/10.3762/bjnano.5.189

Jamal, M., Kamali, S. N., Yazdani, A., & Reshak, A. H. (2014). Mechanical and thermodynamical properties of hexagonal compounds at optimized lattice parameters from two-dimensional search of theequation of state. *RSC Advances*, *4,* 57903-57915. https://doi.org/10.1039/C4RA09358E

Janke, C. (2008). *Density Functional Theory modelling of intrinsic and dopant-related defects in Ge and Si*. PhD Physics Thesis, University of Exeter.

Lee, S. K. (2007). *Preparation and characterization of Silicon Dioxide nanoparticles and thin films*. B.Sc. Dissertation, University Malaysia Sarawak, Malaysia.

Micoulaut, M., Cormier, L., & Henderson, G. S. (2006). *The structure of amorphous, crystalline and liquid GeO.* Retrieved from https://arxiv.org/pdf/cond-mat/0609730.pdf

Nazmul I., & Dulal C. G. (2012). On the electrophilic character of molecules through Its relation with electronegativity and chemical hardness. *Int. J. Mol Sci*., *13*(2), 2160-2175.https://doi.org/10.3390/ijms13022160

Nikolaos, P. K., George, C. S., Nikiforidis, G., Shanawer, N., & Aristides, D. Z. (2016). AB Initio study and design of silicon and silicon-based nanoparticles for controlled drug delivery. *International Journal of Biology and Biomedical Engineering*, *10*, 16-24.

Popovic, D. M., Milosavljevic, V., Zekic A., Romcevic, N., &Daniels, S. (2011). Raman scattering analysis of silicon dioxide single crystal treated by direct current plasma discharge. *Appl. Phys. Lett., 98*, 051503. https://doi.org/10.1063/1.3543838

Robertson, J. (2004). High dielectric constant oxides. *Eur. Phys. J. Appl. Phys*., *28*, 265-291. https://doi.org/10.1051/epjap:2004206

Sahnoun, M., Daul, C., Khenata, R., & Baltache, H. (2005). Optical properties of germanium dioxide in the rutile structure. *The European Physical Journal B*, *45*(4), 455-458. https://doi.org/10.1140/epjb/e2005-00219-y

Stewart, R. F., & Craven, B. M. (1993). Molecular electrostatic potentials from crystal diffraction: the neurotransmitter y-Aminobutyric acid. *Biophysical Journal*, *65*, 998-1005.

Taura, L. S., Ndikilar, C. E., & Muhammad, A. (2017), Modeling the structures and electronic properties of Uraciland Thymine in gas phase and water, *Modern Applied Science,11*(11), 01-11.

Wang, L. S., Desai, S. R., Wu, H., & Nichloas, J. B. (1997). Small silicon oxide clusters: chains and rings. *Z. Phys. D*, *40*, 36-39.

Yuhai, T., & Tersoff, J. (1999). *Structure and energetics of the Si-SiO_2 interface*. arXiv:cond-mat/9903424v1